Remote Sensing of Environment 122 (2012) 166–174

Contents lists available at SciVerse ScienceDirect

Remote Sensing of Environment

journal homepage: www.elsevier.com/locate/rse

Detecting post-fire salvage logging from Landsat change maps and national fire survey data

Todd A. Schroeder [a,*], Michael A. Wulder [b], Sean P. Healey [a], Gretchen G. Moisen [a]

[a] U.S. Department of Agriculture Forest Service, Rocky Mountain Research Station, Ogden, UT, 84401, USA
[b] Canadian Forest Service (Pacific Forestry Centre), Natural Resources Canada, Victoria, British Columbia, V8Z 1M5, Canada

ARTICLE INFO

Article history:
Received 3 May 2011
Received in revised form 22 September 2011
Accepted 7 October 2011
Available online 10 February 2012

Keywords:
Post-fire salvage logging
Landsat time series
Change detection
National fire survey data

ABSTRACT

In Canadian boreal forests, wildfire is the predominant agent of natural disturbance often with millions of hectares burning annually. In addition to fire, nearly one quarter of Canada's boreal forest is also managed for industrial wood production. Post-fire logging (or salvage harvesting) is increasingly used to minimize economic losses from fire, notwithstanding that the ecological impacts of successive disturbance events remain poorly understood. Improved monitoring and management of post-fire environments will require new information regarding the location and timing of past operations. In this paper we present and evaluate a data integration approach for detecting spatial and temporal trends in post-fire logging. Here we utilize a series of maps relating timing and extent of burned area (from the Canadian Large Fire Database) and year of harvest (from Landsat change detection) to identify occurrences of post-fire logging between 1987 and 2008 for a portion of boreal forest located in central Saskatchewan, Canada. Using a design-based, stratified random sampling framework we found that 68% (95% confidence interval (CI) [53 to 84%]) of the detected post-fire logging was correctly classified, such that both fire and clearcutting disturbances were positively verified by the reference data. The majority of map error resulted from spectral confusion between harvested areas and rock outcroppings exposed by fire and from mislabeling harvested unburned islands as post-fire logging. To add further confidence to our classification accuracy, we also found that mapped post-fire logging displayed similar temporal trends over a ten year period as salvage volume reported for a forest management area partially contained within the study area. Based upon the significant relationship between these estimates ($r = 0.97$, $p < 0.001$) and the good degree of observed map accuracy, we believe that the presented approach offers a viable and flexible option for characterizing the spatial and temporal dynamics of post-fire logging in boreal forests. Maps which reliably identify areas of post-fire logging stand to improve our capacity to manage and model the ecological impacts associated with multiple disturbance events.

Published by Elsevier Inc.

1. Introduction

The boreal forests of Canada represent one of the most extensive forest ecosystems on the planet, with the forest ecosystem providing both economic opportunities and environmental goods and services. Harvesting activities are common in the more accessible and productive southern areas of the boreal, with fires acting as the key agent of disturbance in more northerly regions (Masek et al., 2011). In addition, the boreal forest also plays an important role in the cycling and storage of carbon, while at the same time providing habitat to a wide range of species. The forest use, conditions, and patterns vary regionally and largely by topography and latitude (Wulder et al., 2011). These forests are among the few globally which are still primarily shaped by natural processes (Schmiegelow et al., 2006). Of the natural disturbance agents occurring in boreal forests (e.g., disease, insects, extreme weather), wildfire is the most prevalent averaging over 2 million ha burned annually, with some years exceeding 7 million ha (Stocks et al., 2003). Fire return intervals are typically around 50 to 150 years (Payette, 1992), with longer intervals typically found in the more moist forests of eastern Canada. Shifts in fire regime over the last several decades have given way to increases in both annual burned area and frequency of large fire events (Kasischke & Turetsky, 2006) with increases in fire frequency and intensity expected to accompany climate change (Easterling et al., 2000).

Although fire is an essential component in the boreal system (Wulder et al., 2007), it often conflicts with forest management, as nearly one quarter of Canada's boreal forest is also subject to harvesting activities aimed at industrial wood production. Across the Canadian boreal region, timber allocations (e.g., annual allowable cut) are often made with little to no consideration of risk posed by wildfire (Schmiegelow et al., 2006). Thus, when valuable timber resources are burned, forest managers often rely on post-fire logging (commonly referred to as salvage harvesting) as a means of gleaning some

* Corresponding author at: U.S. Department of Agriculture Forest Service, Rocky Mountain Research Station, 507 25th St., Ogden, UT, 84401, USA. Tel.: +1 801 625 5690.
E-mail address: tschroeder@fs.fed.us (T.A. Schroeder).

0034-4257/$ – see front matter. Published by Elsevier Inc.
doi:10.1016/j.rse.2011.10.031

economic benefit from the burned forest. Other reasons cited for undertaking timber salvage include reduction of fuel loads, promotion of regeneration, and public safety; although, competing points of view regarding the impact of these applications do exist (Donato et al., 2006). Rates of salvage harvest are variable based on: land ownership, geographic location, supply and demand of timber, market price fluctuations, and distance from existing road networks. Resource management decisions to salvage harvest are often made in the 2 years after a wildfire or other disturbance has occurred, rather than applying a pre-formulated salvage harvesting policy (Lindenmayer et al., 2004).

Although logging is a frequently employed silvicultural treatment used after natural disturbance, the ecological consequences of successive disturbances occurring over a short period of time are not well understood or agreed upon. For example, some have found post-fire logging both an effective way to reduce future fire risk through removal of dead standing trees (Ne'eman et al., 1997) and a way to hasten ecosystem recovery through re-establishment of favorable tree species (Sessions et al., 2004). Alternatively, others have found that areas subject to post-fire logging reburn more severely than similar unmanaged areas (Thompson et al., 2007) and that post-fire logging hinders regeneration by removing seed-bearing branches (Greene et al., 2006) and by destroying naturally recruited seedlings (Donato et al., 2006). Given the disparity of findings regarding the ecological impacts of post-fire logging, it is important that resource managers be able to locate these areas for further monitoring. Carbon monitoring efforts would also benefit from improved detection of post-fire logging as there are important differences in the fate of forest carbon affected by fire, logging, and fire followed by logging (Mkhabela et al., 2009). Existing carbon monitoring approaches have the capacity to incorporate salvage processes (e.g., Kurz et al., 2009), highlighting the potential benefit of more spatially and temporally specific mapping of post-fire logging. Further, the successional trajectory taken by a particular stand will vary depending on the nature of disturbance (Taylor & Chen, 2010); therefore it is important to identify salvaged locations so as to ensure proper allometric conversion to volume. Agencies responsible for forest monitoring and reporting also need to be mindful of forest salvage to avoid tabulating a given location as fire in one year and fire in a latter year, effectively double counting the disturbed area.

Satellite remote sensing offers an affordable and effective tool for monitoring forest change over large areas. At regional scales, the Landsat suite of optical satellites are particularly useful for monitoring forest change as they have unprecedented historical coverage (40 years of observations), as well as the necessary spatial (30 m pixels) and spectral (7 bands including shortwave-infrared) resolutions which permit capture of most natural and managed disturbance events (Cohen & Goward, 2004; Wulder et al., 2008). The opening of the Landsat archive (Woodcock et al., 2008) has led to development of new change detection techniques which can simultaneously consider the signal from multiple, annually acquired images (Kennedy et al., 2009; Lambin & Linderman, 2006). This multi-temporal signal has been used to study forest recovery (Schroeder et al., 2007), as well as to characterize the timing, extent and magnitude of several types of forest disturbance (Huang, Goward et al., 2010; Kennedy et al., 2010). Both abrupt events (i.e., clearcutting) and slower trends (i.e., insect infestation, see Goodwin et al., 2008) can be reliably captured; however detection of multiple successive disturbances has proven challenging even with a high degree of user intervention. The difficulty arises when an initial disturbance (in this case from fire) diminishes canopy reflectance to the point where it cannot be spectrally separated from the second, more discrete disturbance of clearcutting (Healey et al., 2006). Spectral confusion can be especially high when two disturbances occur in rapid succession, as is often the case with salvage motivated operations.

Given these difficulties it is not surprising that the published literature contains few studies which use remote sensing to monitor impacts of salvage logging. The only located example uses Landsat imagery to study rates and landscape patterns of salvage logging after a jack budworm outbreak in northern Wisconsin (Radeloff et al., 2000). In this study salvage logging was mapped using post-classification comparison of forest clearcut maps derived with Landsat imagery acquired before, during and after the insect outbreak. The clearcuts mapped "after" the start of the outbreak which fell within boundaries set by aerial sketch maps were taken to represent salvage, even though some of these areas may not have been defoliated prior to harvesting. Although the forest clearcut maps were found to be of high quality, no attempt was made to validate the accuracy of salvage detection, especially as it pertained to successful detection of both disturbances. Here our objective is to determine if a similar data combining approach can be used to detect both disturbances associated with post-fire logging.

To address this objective we first map post-fire logging over a 21-year period for an area of boreal forest located in central Saskatchewan, Canada. Using a GIS overlay we compare fire perimeter polygons derived by the Canadian national fire survey (Amiro et al., 2001; Stocks et al., 2003) with forest clearcuts mapped with Landsat change detection (Schroeder et al., 2011). In places where the data sets overlap it is possible to label the timing of each harvest according to the number of years before or after a fire. As both data sets are temporally comprehensive, we elected to define post-fire logging as the clearcuts which were harvested within 5 years after a fire. The accuracy of post-fire logging detection is evaluated using a design-based sample of user interpreted reference points and with provincial salvage volume statistics reported for a forest management area partially contained within the study area. The sample point validation is specifically designed to quantify the method's capacity for detecting both fire and harvest disturbances, while at the same time accounting for error caused by omission of post-fire logging outside of the fire boundaries. On the other hand, comparison with provincial salvage statistics offers a relative measure of temporal consistency of detected salvage across time. In closing, we discuss the results in the context of potential future applications, including expansion of maps to larger spatial extents and different forest types.

2. Methods

2.1. Study area

Located in central Saskatchewan, the study area (represented by the 185 km × 185 km footprint of Landsat path 37 row 22) lies primarily within the Boreal Plains ecozone (Marshall & Shut, 1999) (Fig. 1). Here warm summers and cold winters give way to a moist climate where precipitation averages between 400 and 500 mm annually (Lands Directorate, 1986). The topography is mostly flat to mildly sloping with elevations ranging from 600 to 800 m above sea level. The predominately dark gray and gray luvisol soils (Morrison & Kraft, 1994) sustain a diverse array of tree species. Drier, well drained sites are typically occupied by mixed woods such as trembling aspen (*Populus tremuloides*) and white spruce (*Picea glauca*), whereas jack pine (*Pinus banksiana*) and black spruce (*Picea mariana*) often dominate drier sites with coarsely textured soils. Deciduous trees such as white birch (*Betula papyrifera*) and balsam poplar (*Populus balsamifera*) are also widely distributed. In poorly drained areas, bogs and fens house open expanses of low lying sedge vegetation mixed with sparse, discontinuous cover of species such as tamarack (*Larix laricina*). According to the Landsat-based, Canada wide EOSD land cover map (Wulder et al., 2008) the study area is approximately 84% forested. The most common disturbances in this region are from wildfire and harvesting operations.

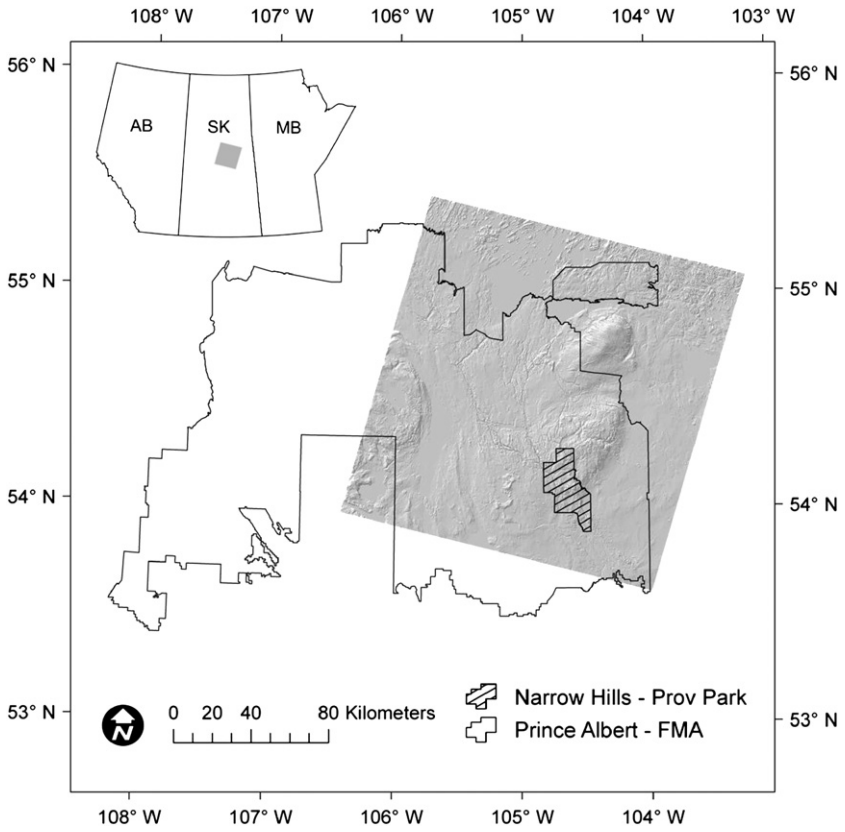

Fig. 1. Location of Landsat path 37 row 22 study area (gray shading) and Prince Albert Forest Management Area (PA-FMA) in central Saskatchewan, Canada.

2.2. Landsat forest clearcut map

The forest clearcut map was produced in a previous study (see Schroeder et al., 2011) for a portion of boreal forest located within Landsat path 37 row 22 (Fig. 1). For this scene 16 growing season (May–September) Landsat TM and ETM+ images were acquired between 1986 and 2008 (Table 1). Prior to classification the images, which mostly fell on an annual time step, were pre-processed using the following steps. First, the images were ortho-rectified and converted to surface reflectance using the Landsat Ecosystem Disturbance Adaptive Processing System (LEDAPS; Masek et al., 2006). Then, to minimize the impact of sun–sensor–view angle effects the images were normalized to a common reference scene. This entailed locating pseudo-invariant features (i.e., temporally stable areas of reflectance) with the iterative multivariate alteration detection (MAD) algorithm (Canty & Nielsen, 2008). The stable bright and dark pixels identified by MAD were used along with band-wise regression to match each image to the reference scene (Schroeder et al., 2006). Areas of cloud and cloud shadow were masked using the algorithm of Huang, Thomas et al. (2010), then filled using an interpolation of the temporally nearest clear observations (see Eq. 5, Huang, Goward et al., 2010).

Table 1
Landsat images used to develop the path 37 row 22 time series.

Sensor	Date
TM	5/23/1986
TM	8/30/1987
TM	9/4/1989
TM	8/22/1990
TM	9/10/1991
TM	6/27/1993
TM	9/1/1994
TM	6/17/1995
TM	9/10/1997
TM	8/28/1998
ETM	7/22/1999
ETM	8/12/2001
TM	8/23/2002
TM	8/12/2004
TM	9/3/2006
TM	9/24/2008

After pre-processing, the images were classified into categories of wildfire and clearcut disturbance using an RGB color composite change detection approach (Sader & Winne, 1992; Wilson & Sader, 2002). This involved simultaneously projecting different dates of imagery through the Red, Green and Blue color channels so that major changes in forest cover appeared in unique shades of primary (RGB) and complimentary (yellow, magenta, cyan) colors. Band 5 (B5) images were used as the shortwave-infrared region has proven useful for detecting forest disturbance (Cohen & Goward, 2004; Healey et al., 2006; Kennedy et al., 2007). Using the concepts of color additive theory the spectral changes observed on screen were interpreted to reflect the timing and cause of forest disturbance. Based on these interpretations a guided approach was used to locate and digitize representative areas of disturbance at each period of the time series. The developed multi-temporal signatures, which contained thousands of pixels per year and disturbance type, were used along with a minimum distance to means supervised classifier to map year and cause of disturbance. Based on the mapping objectives, areas which had undergone multiple disturbances were coded to reflect the year of first disturbance. A similar RGB compositing approach was also used to collect a separate, non-overlapping stratified sample of reference points ($n=960$) for the purpose of validating the final disturbance map.

Overall, the forest disturbance map (including both fire and clearcut classes) was found to have high overall accuracy (kappa = 0.91). Although accuracy was high, a small portion of map error was attributed to mislabeling areas which had undergone multiple disturbances. This included salvaged areas as spectral confusion arose when fire was followed soon after by clearcutting. This spectral

confusion is illustrated by the B5, multi-temporal forest disturbance signatures presented in Fig. 2. Developed with hand selected pixels from the path 37 row 22 time series, these signatures highlight the high degree of spectral separability between fires (green line) and clearcuts (red line) in the shortwave-infrared spectral region. Because B5 reflectance is sensitive to forest structure, shadowing and canopy moisture (Horler & Ahern, 1986), different amounts of canopy removal (i.e., fire = variable canopy removal; clearcutting = full canopy removal) resulted in different magnitudes of spectral change. Ultimately, it was the initial difference in magnitude of spectral change which permitted accurate classification of the fire and clearcut disturbances. Since training signatures were not explicitly developed for areas of salvage logging (blue line), misclassification occurred due to the similarity between these signatures and those from clearcutting several years after a fire (red line). While this mislabeling was considered an error in the context of mapping initial disturbance (see Schroeder et al., 2011 for more information), it is not detrimental to the data integration approach used here since a second data set is used to identify the timing, extent and location of wildfires. Prior to analysis, the clearcut portion of the disturbance map was smoothed with a 5×5 majority filter to remove noise associated with single misclassified pixels. The final forest clearcut map used in the GIS overlay is presented in Fig. 3a.

2.3. Fire perimeter map

The Canadian Large Fire Database (LFDB, Amiro et al., 2001; Stocks et al., 2003) contains data collected by provincial, territorial and federal agencies on wildfires greater than 200 ha which have occurred across Canada between 1980 and 2006 (based upon annual updating).

The information includes fire ignition dates and causes, estimates of burned area, and applied suppression efforts, as well as spatial locations in the form of point and polygon GIS coverages. While older data exists, maps produced since 1980 benefit from the advent of coarse spatial resolution mapping of fires (see Fraser et al., 2004), leading to increased consistency over previous methods which included air photo-based or visual survey practices. Fire mapping efforts in Canada are a partnership between provincial and federal agencies and are well summarized in de Groot et al. (2007). Culled from this national database, we use the co-located fire perimeter polygons (Fig. 3b) to identify areas which have been burned by wildfire. To facilitate implementation of the GIS overlay approach we rasterized the vector fire perimeters (coded to reflect year of fire) to match the spatial extent and grid cell resolution (i.e., 28.5 m) of the Landsat clearcut map.

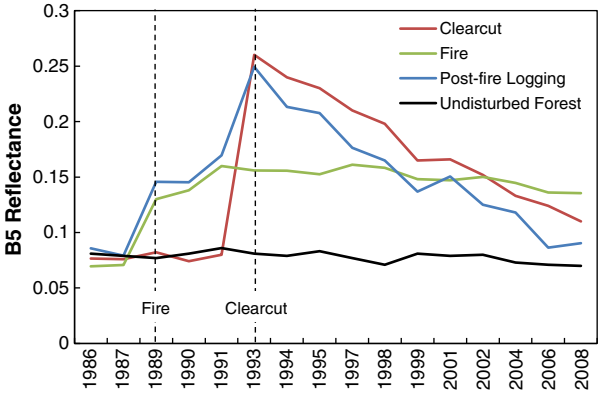

Fig. 2. Landsat band 5 (B5) multi-temporal signatures of disturbance. Dashed lines indicate the onset of fire and clearcutting.

2.4. GIS detection of post-fire logging

Areas of post-fire logging are identified using a GIS approach where year of fire from the LFDB perimeter polygons is spatially subtracted from year of clearcutting from the Landsat clearcut map. This simple spatial overlay is used to identify the forest clearcuts which are spatially co-located with the LFDB fire perimeters. Given the dense temporal information contained within each data set, the identified clearcuts occurred anywhere between 19 years before, to 21 years after fire. After performing the GIS overlay a decision must be made regarding which of the identified clearcuts to call post-fire logging. A plot of area disturbed by clearcutting in relation to timing of wildfire (Fig. 4) shows that the majority of post-fire logging occurs within the first few years after fire. Based on this information, along with the fact that trees have a limited post-fire window of merchantability which varies regionally and often by moisture conditions, we elected to use the clearcut areas disturbed between 0 (i.e., burned and cleared in the same year) and 5 years after fire as our post-fire logging class. Areas which met these spatial and temporal criteria were coded to reflect year of post-fire logging. The remaining harvest areas were labeled as non-salvage clearcuts.

2.5. Reference data

2.5.1. Sample points

Obtaining reference data for a complex multi-disturbance phenomenon such as post-fire logging is difficult, especially when considered over a twenty year time period. As existing data sets often lack sufficient temporal and spatial detail to adequately assess map reliability over space and time, studies are increasingly relying on user interpreted sample points to validate forest change maps (Cohen et al., 2010; Thomas et al., 2011). While ancillary data such as air photos are often used to augment interpretation, in many cases the images which make up a Landsat time series are used as the primary data source from which reference information is collected. Here we use the Landsat time series described in Section 2.2, along with high resolution air photos (from Google Earth: earth.google.com) to interpret the presence or absence of post-fire logging for a series of randomly selected sample points. These points were derived separately from those used to validate the forest clearcut map (described previously in Section 2.2), and are therefore not spatially co-located.

Limitations of our GIS-based approach include not being able to detect post-fire logging outside the fire perimeter boundaries and the assumption that all area within each fire perimeter is actually burned by wildfire. Thus, to understand the contribution of these limitations to overall map error it is imperative that reference sample points be well distributed over all portions of the study area (excluding water). To accomplish this we employ a stratified design using 4 strata classes (Table 2) defined by different combinations of the fire and clearcut raster maps. The 4 sampling strata consist of: 1.) Areas mapped as post-fire logging in Section 2.4, 2.) Areas inside the fire perimeters which were not identified as post-fire logging, 3.) Areas of mapped clearcuts which fall outside of the fire perimeters, and 4.) Areas with no mapped burning or clearcutting. For the purpose of accuracy assessment, post-fire logging areas which were burned and clearcut in the same year (i.e., time zero in Fig. 4) were labeled as strata class 2, as it is not possible to conclusively verify the occurrence of both disturbances when they are simultaneously captured by the same Landsat image.

Using a map of the 4 strata classes we randomly assigned 300 sample points across the study area, with the requirement that each class be assigned a minimum of 50 points (see Table 2 for class sample sizes). To minimize errors associated with interpreting single pixels the sample points were randomly placed using a window majority rule which required at least 6 of 9 pixels in a 3×3 block to be of

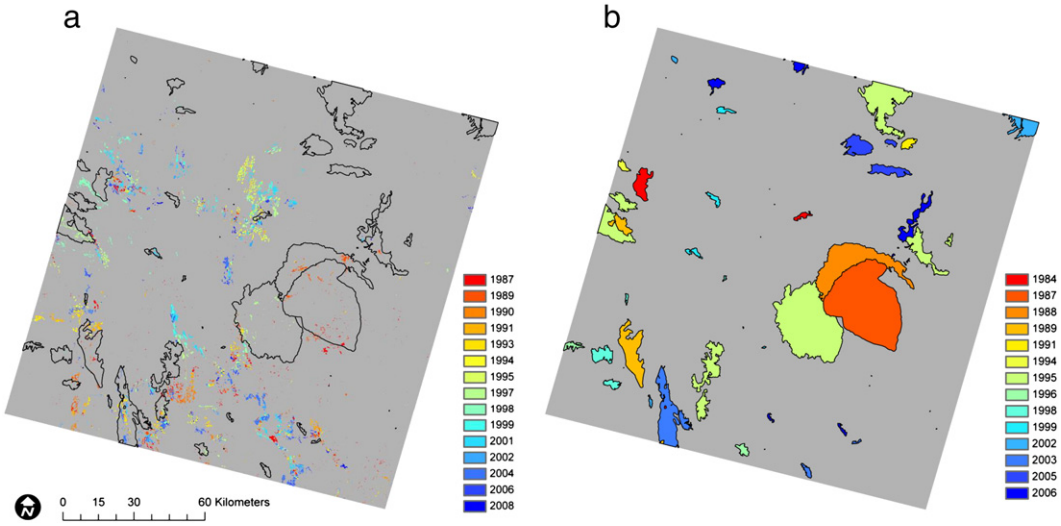

Fig. 3. Raster maps used to detect post-fire logging include a.) forest clearcuts from Landsat change detection and b.) fire perimeter polygons from the Canadian Large Fire Database (LFDB).

the same strata class. Once the sample points were randomly placed, each was given a reference label based on the visual inspection of individual Landsat images (arranged in chronological order) and data appropriate high resolution imagery (as present in Google Earth). The assigned reference labels correspond to the disturbance dynamics of burning and cutting which are assumed to occur in each of the strata classes (see reference label descriptions in Table 2).

In most situations the burning and cutting dynamics could be confidently ascertained from inspection of the Landsat time series; however, in cases where this was not possible, a fifth reference label was used to indicate that interpretation was inconclusive. Excluding the inconclusive samples, the interpreted sample points are used to generate an error matrix, which is adjusted for disproportionate class area sizes using the equation for stratified random samples found in Table 21.2 of Stehman and Foody (2009). The weighted error matrix is used to calculate overall accuracy (i.e., the sum of the primary matrix diagonal/total number of sample points) and Cohen's kappa (Landis & Koch, 1977), a conservative metric of classification accuracy which takes into account the amount of agreement expected by random chance. Individual class accuracies are evaluated using commission and omission errors, which are obtained by subtracting 100% from the user's and producer's accuracies respectively (Janssen & van der Wel, 1994). The producer's accuracy measures how well the reference samples have been classified (including errors of omission), whereas the user's accuracy gages how well the map represents the actual conditions on the ground.

As primary interest lies with the accuracy of the post-fire logging class, we focus on evaluating its user's accuracy, or the proportion of mapped pixels which are correctly assigned according to the interpreted reference samples. When evaluating accuracy estimates it is necessary to account for the uncertainty attributable to sampling variability. Therefore we calculate the error of the post-fire logging class using the variance estimation formula for user's accuracy found in Table 21.3 of Stehman and Foody (2009). A 95% confidence interval is constructed as the parameter estimate, plus or minus two standard errors (here the standard error is taken as the square root of the variance estimator). Lastly, we adjust the area of post-fire logging according to the map error using class marginal proportions as in Card (1982).

2.5.2. Provincial salvage statistics

In addition to validating the post-fire logging map with the reference sample points, we also compare its estimates of clearcut area (ha) with provincial estimates of salvage harvest volume (m^3) reported for years 1999–2008 (Saskatchewan Ministry of Environment, 2009). The Saskatchewan provincial report includes detailed numbers for the 32,000 km^2 Prince Albert Forest Management Area (PA-FMA) which is partially covered by our study area

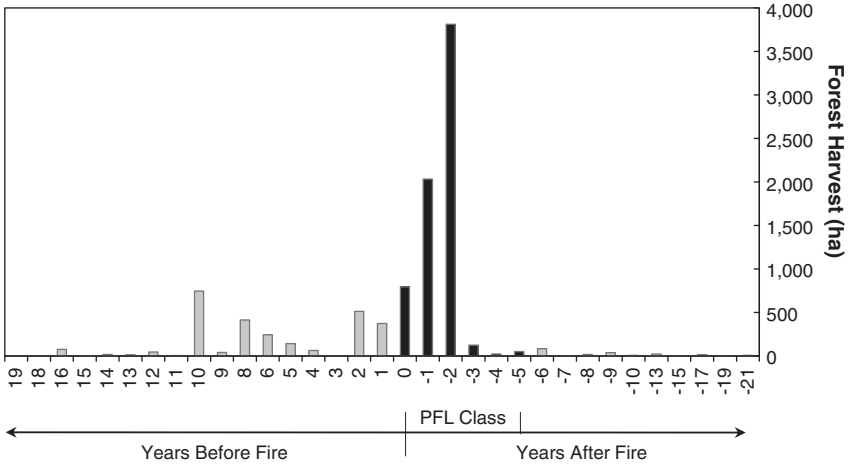

Fig. 4. Area disturbed by forest clearcutting (ha) in relation to timing of wildfire. Time intervals used to define the post-fire logging (PFL) class are shaded black.

Table 2
Sampling strata and associated label codes used in the collection of reference sample points. Abbreviations are: CC = clearcut, FP = fire perimeter.

Strata class:	Strata definition:	Reference label:	n
1	Inside FP and CC 1–5 years after fire	Burned–cut	38
2	All other areas inside FP	Burned–not cut	63
3	CC outside FP	Not burned–cut	53
4	Not CC outside FP	Not burned–not cut	134
5	–	Inconclusive	12
Total			300

(see Fig. 1). To facilitate comparison we restrict the mapped estimates of post-fire logging to the PA-FMA region. In addition, we combined the yearly provincial estimates of salvage volume to account for gaps of up to 2 years in the Landsat time series. After adjusting the data to account for these spatial and temporal differences we determine the similarity of the two data sets using bar plots and strength of linear dependence as calculated by Pearson's correlation coefficient (r).

3. Results

3.1. Post-fire logging map

The GIS overlay procedure, which combined the spatial and temporal dynamics of the forest clearcut map and the fire perimeter data, successfully identified areas of post-fire logging within the study area. A detailed example of the detected post-fire logging is presented in Fig. 5. The Landsat image captured immediately after the fire (left column) clearly shows burned vegetation as green within the yellow LFDP burn perimeter, as opposed to unburned vegetation (including unburned islands) which appears in various shades of red. The Landsat image acquired one time step later shows clearcuts as bright cyan (center column) and non-harvested burned areas in lighter shades of red, green and cyan. Newly installed roads are clearly visible in the post-burn Landsat image. The post-fire logging map (right column) correctly captures the areas inside the fire perimeter which appear most impacted by clearcutting.

After adjusting for error, the map indicates that 4148 ha of forest were potentially disturbed by post-fire logging during the 21-year period from 1987 to 2008. The dense temporal increment of the classification made it possible to track yearly changes in each disturbance type over a two decade time period. To explore the temporal patterns we derive annual rates of disturbance as the yearly percentage of each category's total disturbance (e.g., yearly post-fire logging disturbance / total post-fire logging disturbance × 100). Thus, for each category (fire, post-fire logging and non-salvage clearcutting) this relative measure represents the percentage of study period disturbance which occurs in a given year (e.g., 38% of the study period's fire occurs in 1995). The annual rates of disturbance (Fig. 6) show that fire imprints the landscape episodically, with large fire events occurring in years such as 1987 and 1995. Despite gaps in the Landsat time series (e.g., 1988, 1992, 1996, 2000, 2003 and 2005) it is apparent that post-fire logging generally mirrors the pattern of fire occurrence with a lag of about 2 years. The episodic nature of fire and post-fire logging stand in sharp contrast to the rate of non-salvage clearcutting, which stays relatively consistent through time.

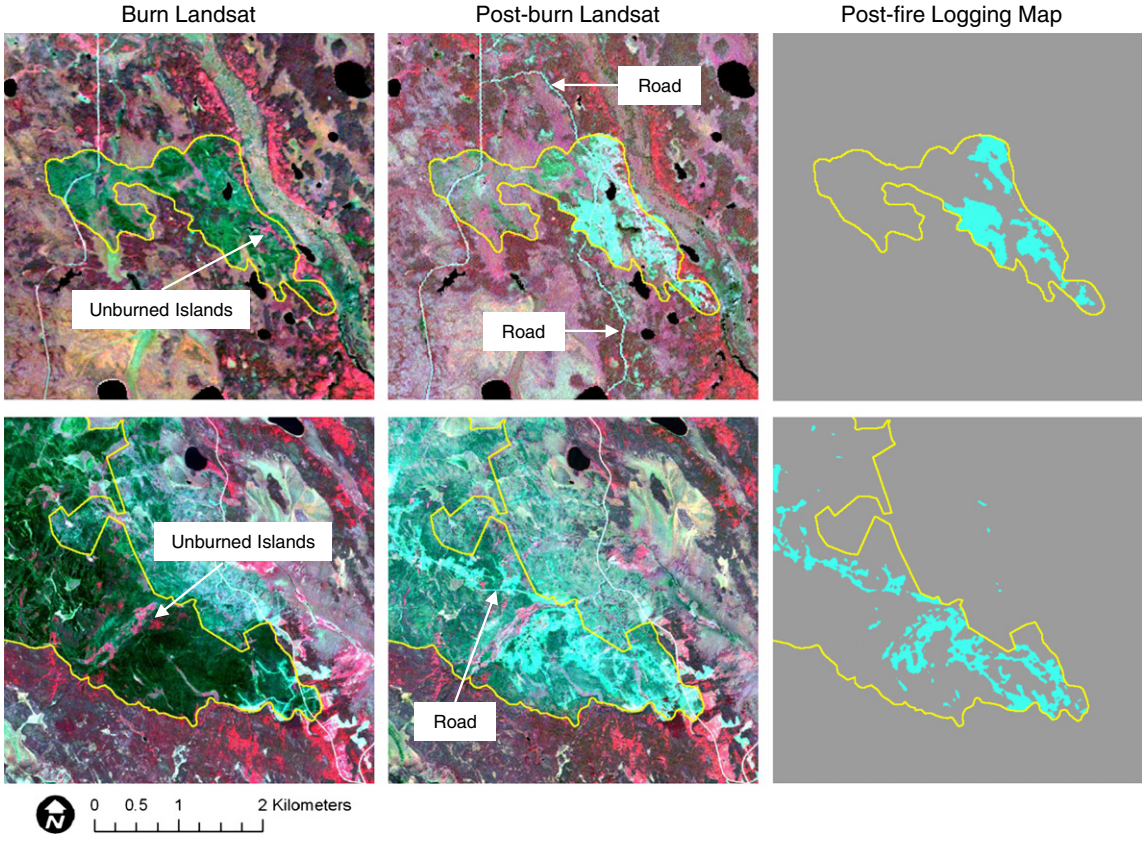

Fig. 5. Examples of post-fire logging detected with the presented GIS modeling approach. The Landsat image (shown in 4, 3, 2 false color) captured immediately after the fire (left column) shows burned vegetation as green within the yellow LFDB fire perimeters. Clearcut areas appear bright cyan in both the post-burn Landsat image (center column) and the post-fire logging map (right column). Unburned islands and newly installed roads are clearly visible in the Landsat images.

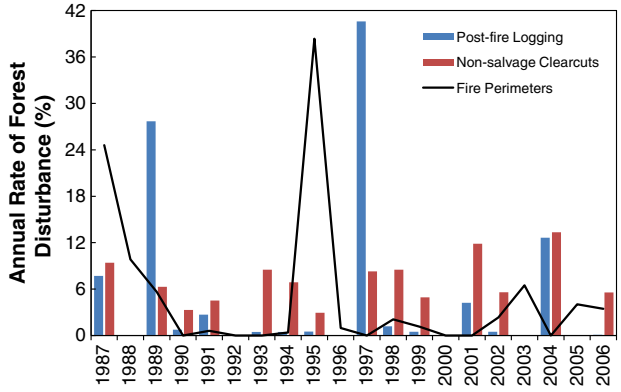

Fig. 6. Annual rates of fire, post-fire logging and non-salvage clearcutting. Rates represent the yearly percentage of each category's total disturbance. For example, 38% of all the study period's fire occurs in 1995. Fire data were available on an annual basis whereas harvest data was subject to gaps in the Landsat time series. Harvests occurring in "gap" years (e.g., 1988, 1992, 1996, 2000, 2003, and 2005) typically were identified with the next available image date. While post-fire logging (blue bars) peaks approximately 2 years after large fire events, non-salvage clearcutting (red bars) occurs at a relatively consistent rate through time.

3.2. Sample point validation

The accuracy of the post-fire logging map was determined with an error matrix (Table 3) derived from the user interpreted sample points. The total number of sample points was reduced from 300 to 288 as the burning and cutting dynamics of 12 of the strata class 1 sample points could not be conclusively verified. Of these 12 samples, 9 (or 75%) were the result of fires which took place in between gaps in the Landsat time series causing the dynamics of fire and forest clearcutting to appear in the same image. The remaining 3 sample points (or 25%) could not be conclusively verified for clearcutting using the available reference data sets. Based on the weighted error matrix (Table 3) we found the overall accuracy of the post-fire logging map to be 95%. According to Landis and Koch (1977), the kappa value of 0.82 indicates a "substantial" level of agreement between the map and reference data even after adjusting for chance agreement. Although overall accuracy and kappa provide a general measure of map quality they are less useful here given our interest in evaluating the post-fire logging class (i.e., strata class 1).

The error matrix (Table 3) reveals that the user's accuracy of strata class 1 is 68.42%. Thus, nearly 70% of the detected post-fire logging was deemed correct by the interpreted sample points. Although this represents a moderately high level of detection accuracy, the high commission error (31.58%) results in broad confidence intervals, such that there is a 95% chance that the accuracy of post-fire logging detection could be as low as 53% or as high as 84%. Some of the observed commission error may be an artifact of our image-based validation. For instance, 5 sample points (or 13% of the strata 1 samples) were classified as post-fire logging but were located in patches or "islands" which from the Landsat perspective appeared unaffected by fire (see unburned islands Fig. 5, left column). Since leaf-on imagery typically resolves disturbances which impact the upper canopy, it is entirely possible that these areas may have experienced some level of understory burning which could not be visually detected, and thus were incorrectly interpreted as unburned. Further, as logging companies are often allocated some proportion of unburned timber as motivation for performing post-disturbance salvage operations, it is also possible that forest managers might want to identify both the burned and unburned areas which were salvaged within a certain period after a fire. In these situations, unburned islands which were harvested post-fire would be considered "salvage" and would therefore not constitute errors.

The second type of commission error in strata class 1 was caused by inclusion of areas which were burned but were not interpreted to be clearcut. These "false positives" were the result of misclassification errors in the forest clearcut map. The misclassification arose because rock outcroppings which were exposed by fire resulted in similar spectral changes (i.e., increased brightness) as areas undergoing clearcutting. This similarity in spectral response led to misclassification, which in turn resulted in 7 sample points (or 18% of the strata 1 samples) being misclassified as post-fire logging. The other major source of map inaccuracy was the 21% commission error for strata class 2 (i.e., areas which were burned but not cut). This error was also caused by our assumption that all areas inside the fire perimeters were burned, although in this case the fact that 13 sample points were found not to have burned did not affect the accuracy of the post-fire logging class.

3.3. Comparison with provincial salvage statistics

To augment the sample point validation, we also evaluate the reliability of post-fire logging detection by comparing the mapped estimates of clearcut area (ha) with provincial salvage volume (m^3) statistics reported for the PA-FMA between 1999 and 2008. The two data sets display comparable temporal patterns of disturbance (Fig. 7) including similar peaks of post-fire salvage logging in 2003–2004 and virtually no detected/reported activity in years 2005–2008. Although trends appear similar, there are noticeable differences in the magnitude of detected disturbance, especially for the 2000–2001 time period. These differences are likely the result of unequal spatial areas (e.g., the study area only covers half of the PA-FMA) and the use of different post-fire definitions and measurement units (i.e., area vs. volume). Despite these data differences we note that the post-fire logging mapped in the 2000–2001 time period was validated with a high degree of certainty (see top row Fig. 5). Despite this difference, the significant linear relationship between the two data sets as determined by Pearson's correlation coefficient ($r = 0.97$, $p < 0.001$) serves as further evidence of the overall reliability of the post-fire logging map.

Table 3
Weighted error matrix used to assess the accuracy of the post-fire logging map. Results are shown as area percentages (e.g., 81.45 refers to 81.45% of the post-fire logging map) with sample point counts in parentheses. Bold numbers indicate where map and reference data are in agreement.

	Reference data				Row total	n	User's	Mapped area (ha)
Strata map	Class 1	Class 2	Class 3	Class 4				
Class 1	**0.18 (26)**	0.05 (7)	0.03 (5)	0.00 (0)	0.26	38	68.42	6063
Class 2	0.00 (0)	**10.61 (50)**	0.00 (0)	2.76 (13)	13.37	63	79.37	315,825
Class 3	0.00 (0)	0.00 (0)	**2.94 (51)**	0.12 (2)	3.06	53	96.23	72,250
Class 4	0.00 (0)	0.62 (1)	1.24 (2)	**81.45 (131)**	83.31	134	97.76	1,967,964
Column total	0.18	11.28	4.22	84.32	100.00	288		2,362,102
n	26	58	58	146				
Producer's	100.00	94.07	69.74	96.59			Overall	95%
Estimated true area (ha)	4148	266,458	99,694	1,991,802			Kappa	0.82

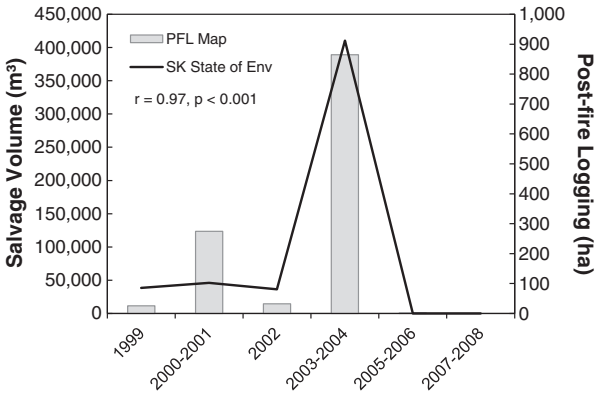

Fig. 7. Estimates of salvage volume (from 2009 Saskatchewan State of the Environment Report; left axis) and area disturbed by post-fire logging (right axis) for the Prince Albert Forest Management Area (PA-FMA). Time periods labeled with 2 years indicate places where yearly salvage volume estimates were combined to match the temporal spacing of the Landsat clearcut map.

4. Discussion and conclusions

In this paper we use a data integration approach to locate potential areas of post-fire logging in boreal forests of Canada. This simple GIS approach is made possible by recent advancements in Landsat time series change detection which permits the spectral separation of clearcut harvests from other types of forest disturbance (Schroeder et al., 2011). To circumvent the difficulties associated with directly detecting multiple disturbances with a Landsat time series, maps of forest clearcutting are combined with national fire burn perimeter data to identify areas of post-fire logging. Using this approach we found that nearly 4148 ha of forest were potentially impacted by post-fire logging during the 21 year period between 1987 and 2008. The post-fire logging map was found to be of good overall quality as determined through validation with manually interpreted sample points (user's accuracy = 68%, 95% CI [53 to 84%]) and via strength of linear correlation with provincial salvage volume statistics ($r = 0.97$, $p \leq 0.001$).

The error in the post-fire logging map was attributed to misclassification of exposed rock outcroppings as clearcuts, and unburned islands as post-fire logging. While the mislabeling of rock outcroppings was caused by spectral confusion inherent in the forest clearcut map, the unburned island errors were a direct result of our strict requirement that both burning and cutting disturbances be positively identified. As the GIS overlay uses fire perimeter data to represent burned area, we recognize that some percentage of the detected post-fire logging will not have burned due to the presence of unburned islands. Based on the error matrix in Table 3, we found that 13% of the post-fire logging samples were not burned prior to harvesting. This finding is noteworthy as forest perimeters are often used to estimate pyrogenic emissions from wildfire. Based on our results the prevalence of unburned islands could be higher than previously assumed by other studies (see Amiro et al., 2001). In the future, Landsat disturbance maps could be used to quantify the proportion of unburned islands and other non-flammable land features (e.g., recent clearcuts, water and urban), leading to more accurate estimates of carbon flux from burn perimeter boundaries.

Whether harvested unburned islands should be considered error in the context of post-fire logging is debatable, and thus depends on the criteria implemented. As we required both fire and harvest disturbances to be evidenced, our validation represents a highly conservative estimate of post-fire logging accuracy. In this case, we are encouraged that nearly 70% of the post-fire logging was correctly classified, such that both fire and clearcutting disturbances were positively verified by the reference data. Equally encouraging was the low omission error, which confirms that the method is not missing areas of post-fire logging which occur outside of the fire perimeter boundaries. Since most salvage logging occurs after large disturbance events, this finding is not entirely unexpected given the reliability with which the fire survey data captures fires greater than 200 ha. Although these large fires represent a small percentage of total fires based upon ignitions, they typically account for more than 97% of the total burned area across Canada (Stocks, 1991). In our study area we found that 92% of the pixels classified as fire in the Landsat disturbance map (described earlier in Section 2.2) fell within the fire perimeter boundaries. This suggests that the fire perimeters are successfully capturing most of the fire locations which are likely to be salvaged.

The reliability of the post-fire logging map is further supported by the significant correlation with the provincial salvage statistics. Although definitive conclusions cannot be drawn given the small sample size ($n = 6$) the statistical relationship (which was based on a ten year period and thousands of mapped pixels) does provide additional verification of the temporal patterns of salvage disturbance resolved by the post-fire logging map. While broad scale patterns of disturbance are useful, the true value of the presented approach lies in the ability to pinpoint stand level salvage cuts for more detailed monitoring. This includes using the Landsat time series to inform on the pre-logging status of salvaged areas (e.g., burned vs. unburned canopy), as well as to track post-salvage forest recovery. Given differences in forest carbon loss and successional recovery after burning and salvage logging (see Fig. 2), the additional monitoring capacity provided by Landsat will allow forest managers the opportunity to better quantify the impacts of these disturbances at both the stand and landscape scales.

Based on the success of the presented example we believe that there is strong potential for expanding this method to other forested areas which have the necessary input raster data sets. As detailed fire perimeter data are now available across Canada (e.g., LFDB Section 2.3) and the United States (e.g., Monitoring Trends in Burn Severity — MTBS, Eidenshink et al., 2007), the broader-scale use of the presented method will depend on the development and accessibility of forest clearcutting maps. Given the distinct temporal response of Landsat SWIR reflectance to full (e.g., clearcuts) and partial (e.g., fire) canopy disturbances (Schroeder et al., 2011) and the emergence of automated techniques for processing and classifying large volumes of Landsat data, we believe that historical forest disturbance maps which attribute full from partial canopy removal will be increasingly available. As uncertainty and agreement regarding the ecological and carbon consequences of post-fire logging is high, methods which can identify these areas for further study and monitoring will be of great benefit to forest managers, government agencies, as well as those interested in better quantifying the carbon effects of multiple disturbances.

Acknowledgments

Funding for this research was provided by the National Aeronautics and Space Administration (NASA) Terrestrial Ecology Program through the North American Forest Dynamics Project. Additional support was provided by the Interior West Region of the U.S. Forest Service's Forest Inventory and Analysis (FIA) program. The participation of Wulder in this research was supported in part by the "EcoMonitor: Northern Ecosystem Climate Change Monitoring" project jointly funded by the Canadian Space Agency (CSA), Government Related Initiatives Program (GRIP) and the Canadian Forest Service (CFS) of Natural Resources Canada.

References

Amiro, B. D., Todd, J. B., Wotton, B. M., Logan, K. A., Flannigan, M. D., Stocks, B. J., et al. (2001). Direct carbon emissions from Canadian forest fires, 1959–1999. *Canadian Journal of Forest Research*, *31*, 512–525.

Canty, M. J., & Nielsen, A. A. (2008). Automatic radiometric normalization of multitemporal satellite imagery with the iteratively re-weighted MAD transformation. *Remote Sensing of Environment*, *112*, 1025–1036.
Card, D. H. (1982). Using known map marginal frequencies to improve estimates of thematic map accuracy. *Photogrammetric Engineering*, *48*, 431–439.
Cohen, W. B., & Goward, S. N. (2004). Landsat's role in ecological applications of remote sensing. *Bioscience*, *54*, 535–545.
Cohen, W. B., Yang, Z., & Kennedy, R. (2010). Detecting trends in forest disturbance and recovery using yearly Landsat time series: 2. TimeSync — Tools for calibration and validation. *Remote Sensing of Environment*, *114*, 2911–2924.
de Groot, W. J., Landry, R., Kurz, W. A., Anderson, K. R., Englefield, P., Fraser, R. H., et al. (2007). Estimating direct carbon emissions from Canadian wildland fires. *International Journal of Wildland Fire*, *16*, 593–606.
Donato, D. C., Fontaine, J. B., Campbell, J. L., Robinson, W. D., Kauffman, J. B., & Law, B. E. (2006). Post-wildfire logging hinders regeneration and increases fire risk. *Science*, *311*, 352.
Easterling, D. R., Karl, T. R., Gallo, K. P., Robinson, D. A., Trenberth, K. E., & Dai, A. (2000). Observed climate variability and change of relevance to the biosphere. *Journal of Geophysical Research*, *105*, 20101–20114.
Eidenshink, J., Schwind, B., Brewer, K., Zhu, Z. L., Quayle, B., & Howard, S. (2007). A project for monitoring trends in burn severity. *Fire Ecology Special Issue*, *3*, 3–21.
Fraser, R. H., Hall, R. J., Landry, R., Lynham, T. J., Lee, B. S., & Li, Z. (2004). Validation and calibration of Canada-wide coarse-resolution satellite burned area maps. *Photogrammetric Engineering and Remote Sensing*, *70*, 451–460.
Goodwin, N. R., Coops, N. C., Wulder, M. A., Gillanders, S., Schroeder, T. A., & Nelson, T. (2008). Estimation of insect infestation dynamics using a temporal sequence of Landsat data. *Remote Sensing of Environment*, *112*, 3680–3689.
Greene, D. F., Gauthier, S., Noël, J., Rousseau, M., & Bergeron, Y. (2006). A field experiment to determine the effect of post-fire salvage on seedbeds and tree regeneration. *Frontiers in Ecology and the Environment*, *4*, 69–74.
Healey, S. P., Cohen, W. B., Zhiqiang, Y., & Kennedy, R. E. (2006). Remotely sensed data in the mapping of forest harvest patterns. In M. Wulder, & S. Franklin (Eds.), *Methods and applications for remote sensing: Concepts and case studies* (pp. 63–84). New York, NY: CRC Press.
Horler, D. N. H., & Ahern, F. J. (1986). Forestry information content of Thematic Mapper data. *International Journal of Remote Sensing*, *7*, 405–428.
Huang, C., Goward, S. N., Masek, J. G., Thomas, N., Zhu, Z., & Vogelmann, J. E. (2010). An automated approach for reconstructing recent forest disturbance history using dense Landsat time series stacks. *Remote Sensing of Environment*, *114*, 183–198.
Huang, C., Thomas, N., Goward, S. N., Masek, J. G., Zhu, Z., Townsend, J. R. G., et al. (2010). Automated masking of cloud and cloud shadow for forest change analysis. *International Journal of Remote Sensing*, *31*, 5449–5464.
Janssen, L. L. F., & van der Wel, F. J. M. (1994). Accuracy assessment of satellite derived land-cover data: A review. *Photogrammetric Engineering and Remote Sensing*, *67*, 1067–1075.
Kasischke, E. S., & Turetsky, M. R. (2006). Recent changes in the fire regime across the North American boreal region — Spatial and temporal patterns of burning across Canada and Alaska. *Geophysical Research Letters*, *33*, L09703.
Kennedy, R. E., Cohen, W. B., & Schroeder, T. A. (2007). Trajectory-based change detection for automated characterization of forest disturbance dynamics. *Remote Sensing of Environment*, *110*, 370–386.
Kennedy, R. E., Townsend, P. A., Gross, J. E., Cohen, W. B., Bolstad, P., Wang, Y. Q., et al. (2009). Remote sensing change detection tools for natural resource management: Understanding concepts and tradeoffs in the design of landscape monitoring projects. *Remote Sensing of Environment*, *113*, 1382–1396.
Kennedy, R. E., Yang, Z., & Cohen, W. B. (2010). Detecting trends in forest disturbance and recovery using yearly Landsat time series: 1. LandTrendr — Temporal segmentation algorithms. *Remote Sensing of Environment*, *114*, 2897–2910.
Kurz, W. A., Dymond, C. C., White, T. M., Stinson, G., Shaw, C. H., Rampley, G. J., Smyth, C., Simpson, B. N., Neilson, E. T., Trofymow, J. A., Metsaranta, J., & Apps, M. J. (2009). CBM-CFS3: A model of carbon-dynamics in forestry and land-use change implementing IPCC standards. *Ecological Modelling*, *220*, 480–504.
Lambin, E. F., & Linderman, M. (2006). Time series of remote sensing data for land change science. *IEEE Transactions on Geoscience and Remote Sensing*, *44*, 1926–1928.
Landis, J. R., & Koch, G. G. (1977). The measurement of observer agreement for categorical data. *Biometrics*, *33*, 159–174.
Lands Directorate (1986). *Terrestrial ecozones of Canada. Ecological land classification no. 19.* 26 pp.
Lindenmayer, D. B., Foster, D. R., Franklin, J. F., Hunter, M. L., Noss, R. F., Schmiegelow, F. A., et al. (2004). Salvage harvesting policies after natural disturbance. *Science*, *303*, 1303.
Marshall, I. B., & Shut, P. H. (1999). *A national ecological framework for Canada — Overview. Ecosystems Science Directorate – Environment Canada, Research Branch – Agriculture and Agri-Food Canada, Ottawa, ON.* 9 pp.
Masek, J. G., Cohen, W. B., Leckie, D., Wulder, M. A., Vargas, R., de Jong, B., et al. (2011). Recent rates of forest harvest and conversion in North America. *Journal of Geophysical Research*, *116*(G00K03). doi:10.1029/2010JG001471.
Masek, J. G., Vermote, E. F., Saleous, N. E., Wolfe, R., Hall, F. G., Huemmrich, K. F., et al. (2006). A Landsat surface reflectance data set for North America, 1990–2000. *IEEE Geoscience and Remote Sensing Letters*, *3*, 68–72.
Mkhabela, M. S., Amiro, B. D., Barr, A. G., Black, T. A., Hawthorne, I., Kidston, J., et al. (2009). Comparison of carbon dynamics and water use efficiency following fire and harvesting in Canadian boreal forests. *Agricultural and Forest Meteorology*, *149*, 783–794.
Morrison, I. N., & Kraft, D. (1994). *Sustainability of Canada's agri-food system — A prairie perspective.* Winnipeg, MB: International Institute for Sustainable Development 168 pp.
Ne'eman, G., Perevolotsky, A., & Schiller, G. (1997). The management implications of the Mt. Carmel research project. *International Journal of Wildland Fire*, *7*, 343–350.
Payette, S. (1992). Fire as a controlling process in the North American boreal forest. In H. H. Shugart, R. Leamans, & G. B. Bonan (Eds.), *A systems analysis of the global boreal forest* (pp. 144–169). Cambridge, UK: Cambridge University Press.
Radeloff, V. C., Mladenoff, D. J., & Boyce, M. S. (2000). Effects of interacting disturbances on landscape patterns: Budworm defoliation and salvage logging. *Ecological Applications*, *10*, 233–247.
Sader, S. A., & Winne, J. C. (1992). RGB-NDVI colour composites for visualizing forest change dynamics. *International Journal of Remote Sensing*, *13*, 3055–3067.
Saskatchewan Ministry of Environment (2009). *Saskatchewan's state of the environment report: State of Saskatchewan's Provincial Forests* (pp. 180).
Schmiegelow, F. K. A., Stepnisky, D. P., Stambaugh, C. A., & Koivula, M. (2006). Reconciling salvage logging of boreal forests with a natural-disturbance management model. *Conservation Biology*, *20*, 971–983.
Schroeder, T. A., Cohen, W. B., Song, C., Canty, M. J., & Yang, Z. (2006). Radiometric correction of multi-temporal Landsat data for characterization of early successional forest patterns in western Oregon. *Remote Sensing of Environment*, *103*, 16–26.
Schroeder, T. A., Cohen, W. B., & Zhiqiang, Y. (2007). Patterns of forest regrowth following clearcutting in western Oregon as determined from a Landsat time-series. *Forest Ecology and Management*, *243*, 259–273.
Schroeder, T. A., Wulder, M. A., Healey, S. P., & Moisen, G. G. (2011). Mapping wildfire and clearcut harvest disturbances in boreal forests with Landsat time series data. *Remote Sensing of Environment*, *115*, 1421–1433.
Sessions, J., Bettinger, P., Buckman, R., Newton, M., & Hamann, J. (2004). Hastening the return of complex forests following fire: the consequences of delay. *Journal of Forestry*, *102*, 38–45.
Stehman, S. V., & Foody, G. M. (2009). Accuracy assessment. In T. A. Warner, M. D. Nellis, & G. M. Foody (Eds.), *The SAGE handbook of remote sensing* (pp. 297–311). London, UK: SAGE Publications Ltd.
Stocks, B. J. (1991). The extent and impact of forest fires in northern circumpolar countries. In J. S. Levine (Ed.), *Global biomass burning. Atmospheric, climatic and biospheric implications*. Cambridge, MA, USA: MIT Press.
Stocks, B. J., Mason, J. A., Todd, J. B., Bosch, E. M., Wotton, B. M., Amiro, B. D., et al. (2003). Large forest fires in Canada 1959–1997. *Journal of Geophysical Research*, *108*, 8149.
Taylor, A. R., & Chen, H. Y. H. (2010). Multiple successional pathways of boreal forest stands in central Canada. *Ecography*, *34*, 208–219.
Thomas, N. E., Huang, C., Goward, S. N., Powell, S., Rishmawi, K., Schleeweis, K., et al. (2011). Validation of North American forest disturbance dynamics derived from Landsat time series stacks. *Remote Sensing of Environment*, *115*, 19–32.
Thompson, J. R., Spies, T. A., & Ganio, L. M. (2007). Reburn severity in managed and unmanaged vegetation in a large wildfire. *Proceedings of the National Academy of Sciences*, *104*, 10743–10748.
Wilson, E. H., & Sader, S. A. (2002). Detection of forest harvest type using multiple dates of Landsat TM imagery. *Remote Sensing of Environment*, *80*, 385–396.
Woodcock, C. E., Allen, R., Anderson, M., Belward, A., Bindschadler, R., Cohen, W., Gao, F., Goward, S. N., Helder, D., Helmer, E., Nemani, R., Oreopoulos, L., Schott, J., Thenkabail, P. S., Vermote, E. F., Vogelmann, J., Wulder, M. A., & Wynne, R. (2008). Free access to Landsat imagery. *Science*, *320*(5879), 1011.
Wulder, M. A., Campbell, C., White, J. C., Flannigan, M., & Campbell, I. D. (2007). National context in the international circumboreal community. *The Forestry Chronicle*, *88*, 539–556.
Wulder, M. A., White, J. C., & Coops, N. C. (2011). Fragmentation regimes of Canada's forests. *The Canadian Geographer*, *55*, 288–300. doi:10.1111/j.1541-0064.2010.00335.x.
Wulder, M. A., White, J. C., Cranny, M., Hall, R. J., Luther, J. E., Beaudoin, A., et al. (2008). Monitoring Canada's forests — Part 1: Completion of the EOSD land cover project. *Canadian Journal of Remote Sensing*, *34*, 549–562.